RSC Advances

ROYAL SOCIETY OF CHEMISTRY

www.rsc.org/advances

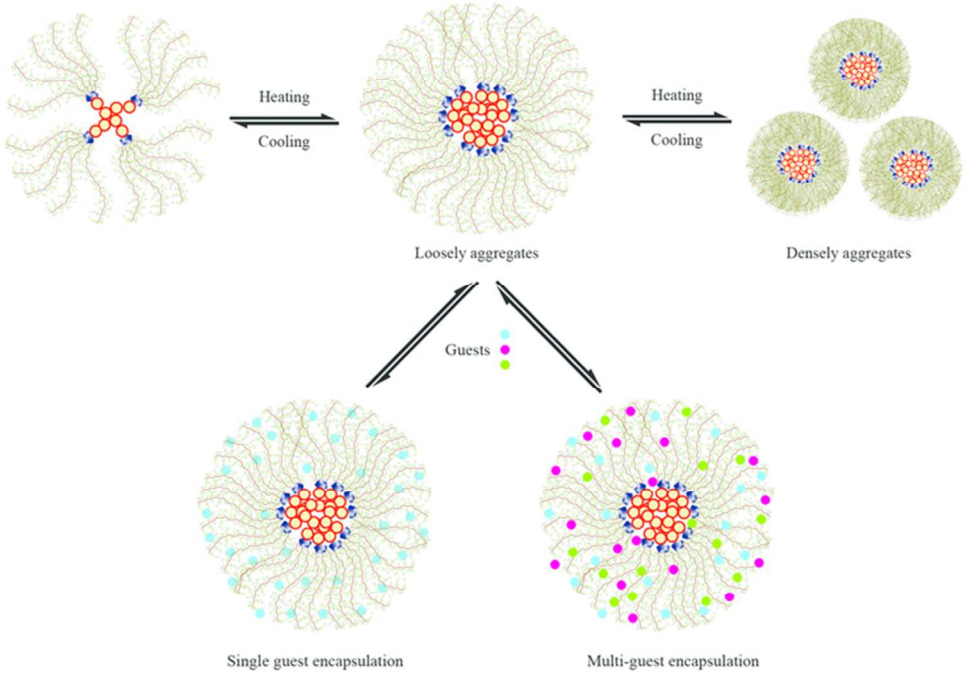

Schematic illustrations of the thermally-induced self-assembly and possible encapsulation behaviors with single or multi-guests for PE-CD-POEGMAs.
64x46mm (300 x 300 DPI)

Synthesis and encapsulation of amphiphilic thermoresponsive star polymer with β-cyclodextrin and hyperbranched poly (oligo (ethylene glycol) methacrylate) as building blocks

Yinwen Li [a, b], Huilong Guo [a, b], Jian Zheng [a, b], Jianqun Gan [a, b], Yan Zhang [a, b], Xiaoxiao Guan [a, b], Kun Wu [a], Mangeng Lu [a,*]

a Key Laboratory of Cellulose and Lignocellulosics Chemistry, Chinese Academy of Sciences; Key Laboratory of Polymer Materials for Electronics, Guangzhou institute of Chemistry, Chinese Academy of Sciences, Guangzhou 510650, PR China.

b University of Chinese Academy of Sciences, Beijing 100039, PR China

Abstract

Novel macromolecular star polymers with triazole and cyclodextrin (CD) segments as branch points and poly(oligo (ethylene glycol) methacrylate) (POEGMAs) as dense hydrophilic branches were synthesized via combination of azide-alkyne click chemistry and atom transfer radical polymerization (ATRP). Firstly, a tetrafunctional linking agent (PETP) was prepared by the reaction of pentaerythritol (PE) and propargyl bromide, and then a four arm β-CD terminated star polymer (PE-CD) was obtained through the click chemistry reaction. Finally, thermally-responsive star polymers (PE-CD-POEGMAs) with PE as the central core, triazole and CD segments as branch points, and POEGMAs as side branches were synthesized by the ATRP of MEO_2MA and OEGMA using PE-CD terminated with bromines as macroinitiators. Study on the thermoresponsivity and morphology of PE-CD-POEGMAs indicated that polymeric nano-aggregates existed as multimolecular micelles and behaved tunable thermosensitivity, which were driven by the strong hydrophobic-hydrophilic interactions in the inner core and outer shell. The encapsulation capacities towards multi-guest molecules were investigated and the results indicated that water soluble guests could be encapsulated by PE-CD-POEGMAs, and the guest encapsulation capacities were derived from the special star

molecular structure properties of PE-CD-POEGMAs and the synergistic encapsulation phenomenon of different guest molecules. This unique amphiphilic star polymer illustrated the potential applications in supramolecular science, drug delivery and other nanotechnology applications.

Introductuiion

Star polymers possess a three-dimensional branched architecture in which chemically different building blocks are linked to a single junction point. Due to their unique structures, star polymers usually exhibit specific properties and potential applications as compared with the corresponding linear block analogues.[1-4] Therefore, star polymers have attracted ever-increasing attention of both scientists and engineers over the past several decades and this field has become a cutting-edge area of polymer and materials research.[5-13]

Stimuli-responsive polymers are often referred to as intelligent polymeric systems because they exhibit reversible property changes between micellar and unimer states in response to changes of external conditions such as pH, temperature, ionic strength and light irradiation, among them, thermoresponsive polymers are potentially interesting for a wide range of applications such as enzyme recycling, protein chromatography, drug delivery, or tissue engineering.[14-22] Classic thermoresponsive polymers exhibit aqueous LCSTs include poly(N-isopropylacrylamide) (PNIPAAm), poly(N-acryloylpyrrolidine), poly(vinyl methyl ether), polypeptides, poly(dimethylaminoethyl methacrylate), which have been by far the most studied and applied.[23-25] Recently, poly(oligo (ethylene glycol) methacrylate)s (POEGMAs) were reported to possess similar or even superior thermosensitivity than PNIPAAms. POEGMAs have good phase transition reversibility and tunable lower critical solution temperature (LCSTs) in aqueous medium, the biocompatibility of POEGMAs is also excellent and attractive. To date, POEGMAs have been widely incorporated into block or star copolymers, polymeric brushes and hydrogels, which endow these materials with more

interesting properties.[26-35] However, to endow star polymers with thermoresponsivity, thermo-responsive monomers or polymeric parts are usually introduced as building blocks; PNIPAAms have been successfully incorporated to various dendrimers or star polymers to form thermo-responsive core-shell nanostructures[36-39], but only few works have been done on introducing POEGMAs into star polymers especially with cyclodextrins(CDs).

Encapsulation is one of the most attractive areas in contemporary supramolecular chemistry and shows great potential in drug delivery, medical diagnostics and materials science. Encapsulation materials include liposomes, chitosan, crown ethers, and cyclodextrins etc. can be defined as functional polymers which show superior encapsulation properties due to their special macromolecule structures and unique physicochemical characteristics.[40-50] amphiphilic linear block or pseudo block polymers are known for their ability to self assemble into polymeric nano-aggregates which have been considered as good candidates for encapsulation investigations and applications, however, the formed nano-aggregates are usually unstable and easily dissociate with altered environmental parameters.[51-53] Compared with amphiphilic linear polymers, amphiphilic nonlinear polymers such as dendrimers, star polymers, and hyperbranched polymers with branched architectures can stably exist as unimolecular micelles or multimolecular micelles in aqueous solution because of their unique chemical structures, and their encapsulation behaviors have been studied and mainly focused on single guest encapsulation.[54-57] Most recently, the encapsulation phenomena of multi-guest molecules using amphiphilic hyperbranched polymers was reported by Tian et al.[58] However, there are still few attentions and researches on encapsulation of amphiphilic thermal responsive star polymer with CDs and hyperbranched POEGMAs as building blocks for multi-guest molecules.

Our research group previously investigated the synthesis and supramolecular self-assembly of a variety of stimuli-responsive POEGMAs with complex architectures. Motivated by

recent attempts in the most attractive areas of encapsulation in contemporary supramolecular host-guest chemistry, herein the synthesis and characterization of thermoresponsive star polymers with PE as the central core, triazole and CD segments as the branch points, and POEGMAs as branches were reported, and the encapsulation behaviors of this newly synthesized star-shaped polymers using rose bengal (RB), levofloxacin lactate (LL), rhodamine B (Rh) and congo red (CR) as guest molecules were investigated in details.

Experimental

Materials

β-cyclodextrin (β-CD) was acquired from Aladdin, China, and purified by recrystallization from water twice prior to use. p-toluenesulfonyl chloride (p-TsCl), sodium azide (NaN_3), pentaerythritol (PE), and propargyl bromide was purchased from Aladdin, China. N, N, N, N, N-pentamethyldiethylenetriamine (PMDETA) and 2-bromoisobutyryl bromide (BIBB) were was purchased from TCI, Japan. Copper(I) bromide (TCI, Japan) was washed with glacial acetic acid in order to remove any soluble oxidized species, then filtered and washed with ethanol, finally dried under vacuum. 2-(2-Methoxyethoxy) ethyl methacrylate (MEO_2MA, Mn=188.2 $g \cdot mol^{-1}$), oligo (ethylene glycol) methyl ether methacrylate (OEGMA, Mn≈ 475-500 $g \cdot mol^{-1}$) were all acquired from TCI, Japan, and passed through short basic alumina column in order to remove inhibitor before use. Rose bengal (RB), levofloxacin lactate (LL), rhodamine B (Rh) and congo red (CR) were all acquired from Aladdin, China, and their molecular structures are shown in Scheme 1. N, N-Dimethylformamide (DMF) was supplied by Sinopharm, China and refluxed over CaH_2 and stored over 4 A^0 molecular sieves. All other reagents were also supplied by Sinopharm, China and used without further purification.

Synthesis of mono-6-OTs-CD (TCD)

β-CD (24 g) was suspended in 180 mL of water, NaOH (2.623 g) in 20 mL of water was added dropwise over 30 min, and reacted under vigorous agitation at 0 ^oC for a period of 1 h.

then p-toluenesulfonyl chloride (4.032 g) in 20 mL of acetonitrile was added dropwise over 1 h, causing immediate formation of a white precipitate. After 3 h of stirring at 20 ^{o}C filtered off unreacted toluenesulfonyl chloride, the solution was neutralized by hydrochloric acid with a pH of 7-8, and the filtrate refrigerated overnight at 4 ^{o}C. The white precipitate was recovered by suction filtration and recrystallization in water for at least three times. The sample obtained was dried at 60 ^{o}C for 48 h in a vacuum oven, and TCD was obtained as a white solid (yield: ≈21.40%). FT-IR (KBr, cm^{-1}): 3388 (s, OH), 2928 (w, CH_2), 1597 (s, Ph). ^{1}H NMR (400 MHz, DMSO-d_6): δ (ppm) 7.42 (2H), 7.74 (2H); 5.65-5.92 (2, 3-OHs of β-CD); 4.75-4.83 (1-Hs of β-CD); 3.28-3.64 (2, 3, 4, 5, 6-Hs of β-CD), 2.42 (CH_3).

Synthesis of mono-6-deoxy-6-azido-b-cyclodextrin (CD-N_3)

CD-N_3 was prepared by the azidation of TCD according to literature procedures with a few modifications. A mixture of β-CD-OTs (6.0 g), dry DMF (20 mL), KI (0.39 g), and NaN_3 (3.05 g) was stirred at 60 ^{o}C for 24 h. After cooling to room temperature, the mixture was precipitated into an excess of acetone, then suction filtration washed with ethanol, cold water and acetone, separately, Last suction filtration and drying for 24 h at room temperature in a vacuum oven yielded a white powder (yield: ≈88%). FT-IR (KBr, cm^{-1}): 2108 (N_3). ^{1}H NMR (400 MHz, DMSO-d_6): δ (ppm) 5.70-5.95 (2, 3-OHs of β-CD); 4.80-4.90 (1-Hs of β-CD); 4.4-4.6 (6-OH of β-CD); 3.20-4.0 (2, 3, 4, 5, 6-Hs of β-CD).

Synthesis of tetrakis (2-propynyloxymethyl) methane (PETP)

Tetrakis (2-propynyloxymethyl) methane (PETP) was prepared as follows. A round-bottomed flask, equipped with a magnetic stir bar, was charged with pentaerythritol (2 g, 0.014 mmol) and NaH (12.5 g, 0.22 mmol). Anhydrous DMF (25 mL) was added by a syringe and the reaction mixture was stirred at 5 ^{o}C for 30 min. Propargyl bromide (20 g, 0.17 mmol) was slowly added over a 120 min period. The reaction mixture was then heated at 40 ^{o}C for 40h. Water (100 mL) was added after cooling, and the mixture was extracted with ethyl acetate.

The organic layers were combined, washed with water and then with brine, and dried over Na_2SO_4. Removal of solvent by evaporation under reduced pressure left a residue that was purified by silica gel column eluting with ethyl acetate to give crude PETP as an orange liguid, then precipitate with cold hexanes an orange solid was obtained (yield: ≈72%). FT-IR (cm^{-1}): ν 3285, 2111. ^{1}H NMR (400 MHz, CDCl3): δ (ppm) 4.12 (8H, HCCCH_2); 3.54 (8H, C(CH_2)$_4$); 2.4 (4H, *H*CCCH2). ^{13}C NMR (CDCl3): δ (ppm) 80.0, 74.0, 69.0, 58.7, 44.7.

Synthesis of four-arm CD-terminated macromonomer (PE-CD)

The synthesis of four-arm CD-terminated macromonomer was accomplished by the click reaction between CD-N_3 and Tetrakis (2-propynyloxymethyl) methane (PETP). A typical procedure was as follows. CD-N_3 (1.12 g), pentaerythritol tetrapropiolate (0.0655 g), and CuBr (0.2875 g) were first dissolved in 20 mL of DMF. The solution was bubbled with nitrogen for 30 min. PMDETA (0.3475 g) was added to the mixture. The mixture was bubbled with nitrogen again for 30 min and sealed under nitrogen atmosphere. The reaction was conducted at 60 ^{o}C for 24 h. The reaction mixture was exposed to air and then precipitated into an excess of diethyl ether. The crude product was dissolved in deionized water and dialyzed against deionized water for 2 d to remove copper catalysts and excess CD-N_3. After freezing drying, a white powder was obtained. Yield: ≈76 %. FT-IR (KBr): 3385 cm^{-1} (O-H); 2870 cm^{-1} (C-H). ^{1}H NMR (DMSO-d6, TMS): δ (ppm) 7.95 (1H, methine proton in 1,2,3-triazole); 5.70-5.95 (2, 3-OHs of β-CD); 4.80-4.90 (1-Hs of β-CD); 4.4-4.6 (6-OH of β-CD); 4.28(8H, HCCCH_2), 3.54 (8H, C(CH_2)$_4$, overlaps with 2,3,4,5,6-H in β-CD).

Synthesis of four-arm CD-terminated macroinitiator (PE-CD-Br$_x$)

PE-CD-Br$_x$ (x≈16 and 48) were synthesized by PE-CD and 2-bromoisobutyryl bromide. PE-CD-Br$_x$ (x≈48) was synthesized as follows: To a 25 ml round-bottomed flask in ice bath, PE-CD (0.493 g, 0.1 mmol), was dissolved in 30 ml DMF and cooled to 0 ^{o}C. 2-bromoisobutyryl bromide (BIBB, 2.76g, 12 mmol) dissolved in 10 ml DMF was then added dropwise to the

solution with magnetic stirring over a period of 1 h at 0 ^{o}C. The reaction temperature was maintained at 0 ^{o}C for another 2 h and then allowed to rise slowly to ambient temperature after which the reaction was allowed to continue for 24 h. The final reaction mixture was precipitated in excess diethyl ether. The white powder precipitate was washed with acetone and water (v/v, 9:1) for at least three times. The purified PE-CD-Br_{48} was collected, washed with acetone, and dried under reduced pressure. Yield: ≈65%. FT-IR (KBr): 3385 cm^{-1} (O-H); 1720 cm^{-1} (C=O). ^{1}H NMR (DMSO-d6, TMS): δ (ppm) 7.95 (1H, methine proton in 1,2,3-triazole); 5.70-5.95 (2, 3-OHs of β-CD); 4.90-4.98 (1-Hs of β-CD); 3.31-3.92 (8H, $C(CH_2)_4$, overlaps with 2, 3, 4, 5, 6-Hs in β-CD); 1.85-1.90 (CH_3).

Synthesis of star polymer (PE-CD-POEGMAs)

PE-CD-POEGMAs (P_1 and P_2) were synthesized by the ATRP of MEO_2MA and OEGMA monomers using PE-CD-Br_x as the macroinitiator. A typical procedure for P_2 is described as follows: the schlenk tube was purged with dry argon for 30 minutes, a degassed mixture of 2-(2-methoxyethoxy) ethyl methacrylate (1520 eq.), oligo (ethylene glycol) methyl ether methacrylate (80 eq.), ethanol (monomers/ethanol ~ 1:1. 5 v/v), PE-CD-Br_{48} (1 eq.) initiator and copper bromide (57 eq.) was added to a Schlenk tube, degassed via three freeze-thaw-pump cycles and back-filled with argon. Then 2, 2-bipyridyl (120 eq.) was added. The mixture was heated at 50°C in an oil bath for six hours. The experiment was stopped by opening the flask and exposing the catalyst to air. The final mixture was diluted in ethanol and passed through a short silica column (60-200 mesh) in order to remove copper catalyst. Then, the filtered solution was diluted with deionized water and subsequently purified by dialysis in water (Roth, ZelluTrans membrane, molecular weight cut-off: 7000). Last, freeze-drying in vacuum PE-CD-POEGMAs was obtained as clear viscous solid. Yield: ≈43%. The synthetic routes employed for the preparation of PE-CD-POEGMAs are shown in scheme 2.

Characterization

Fourier transform infrared (FT-IR) spectra were recorded on a Nicolet 5100 spectrometer by KBr sample holder method in the fundamental region of 400-4000 cm^{-1}. ^1H NMR spectra were obtained on a Bruker DMX-400 spectrometer. Deuterated chloroform ($CDCl_3$), deuterated water (D_2O), or deuterated dimethyl sulfoxide (DMSO-d_6) was used as the solvent. The number-average molecular weight (Mn) and polydispersity index (Mw/Mn) of each polymer were determined at 35 °C using a Waters 1515 size exclusion chromatograph (SEC) equipped with a Waters 2414 refractive index (RI) detector. DMF was used as the eluant and the columns used were the styragel HR_3 and HR_4 columns calibrated by narrow PS standards.

The LCSTs were determined by UV-vis spectroscopy (U-3010 Spectrophotometer), and transmittance of the polymeric aqueous solutions (1 mg/mL) was recorded at temperatures ranging from 20 ^oC to 70 ^oC. The lower critical solution temperature (LCST) of the aqueous polymer solution at specific concentration was determined as the temperature corresponding to 10% decrease in the optical transmittance. The hydrodynamic diameters (Dh) of the capsules and their polydispersity indices (PDI) were determined by dynamic light scattering (DLS) on a Malven Zetasizer Nano System (Nano-zs90). The emulsions were passed through 1.0 μm filters before DLS measurements. The measurements were conducted in a 3.0 mL quartz cuvette, using a 670 nm diode laser, and the scattering angle used was 90°. Each set of Dh and PDI values was the average from five measurements.

Single guest encapsulation

The single guest encapsulation of PE-CD-POEGMAs was measured by fluorescence spectrophotometry. Firstly, RB (5×10^{-4} mol L^{-1}), LL (5×10^{-4} mol L^{-1}), Rh (5×10^{-4} mol L^{-1}) and CR (5×10^{-4} mol L^{-1}) as guest molecules were dissolved in PBS buffer solution with ionic strength equal to 0.1 mol L^{-1} and pH=7.4, respectively. Then, the PE-CD-POEGMAs solution with various desired concentrations ranging from 1.0×10^{-1} mg mL^{-1} to 1.0×10^{-7} mg mL^{-1} were

mixed with the above guest solution, respectively. All mixed solutions were maintained for more than 24 h to ensure the binding equilibrium and then stirred prior to measurement.

Multi-guest encapsulation

The multi-guest encapsulation of PE-CD-POEGMAs was also measured by fluorescence spectrophotometry. The PE-CD-POEGMAs solution with various desired concentrations ranging from 1.0×10^{-1} mg mL^{-1} to 1.0×10^{-7} mg mL^{-1} were mixed together with five multi-guest groups RB+Rh, LL+Rh, CR+Rh, CR+LL+Rh, RB+LL+Rh, respectively. All mixed solutions were maintained for more than 24 h to ensure the binding equilibrium and then stirred prior to measurement. All the solvent used for the solution preparation was PBS buffer solution with ionic strength equal to 0.1 mol L^{-1} and pH = 7.4.

Results and discussion

Synthesis of star polymers (PE-CD-POEGMAs)

To obtain PE-CD-POEGMAs, TCD was first synthesized by using a β-CD monomer according to our previous work.[34] CD-N_3 and Tetrakis (2-propynyloxymethyl) methane (PETP) were synthesized according to literatures with a few modifications. Afterwards, click chemistry was used as a versatile strategy to prepare four-arm CD-terminated star monomer (PE-CD) because of its high specificity, high yield, and near-perfect fidelity. PE-CD was then sequentially modified using 2-bromoisobutyryl bromide to obtain macroinhibitors (PE-CD-Br_x, x≈16 and 48). Lastly, PE-CD-POEGMAs ($P_1$and P_2) were achieved by ATRP using MEO_2MA and OEGMA as the monomers and PE-CD-Br_x as the macroinitiators. Polymeric structures of TCD, CD-N_3, PETP, PE-CD, PE-CD-Br_x and PE-CD-POEGMAs were characterized by FT-IR, ^{1}H NMR, SEC, and MALDI-TOF-MS measurements.

Firstly, as shown in Scheme 2, the synthesis of the four-arm star polymers started from the synthesis of tetrakis (2-propynyloxymethyl) methane (PETP). The synthetic methods of PETP reported in previous literatures are somewhat ambiguous and the results are even

completely contradictory.[60-62] In order to improve the synthetic method and productivity of PETP, treatment of pentaerythritol by our modified method with propargyl bromide and NaH synthesized the target PETP in good yield. The FT-IR and ^{1}H NMR spectra of PETP are shown in Fig. 1 and Fig. 2(a), separately. The chemical shifts at 4.12 (8H, -OCH_2), 3.54 (8H, C(CH_2)$_4$), and 2.43 (4H, CH) were attributed to protons originating from pentaerythritol and propargyl segments. Moreover, in the FT-IR spectrum of PETP, the disappearance of the stretching vibration peak of the hydroxyl group at 3443 cm^{-1}, together with the appearance of the characteristic absorption peaks of alkynyl groups (2111 cm^{-1}, 3285 cm^{-1}) suggested that the terminal hydroxyl groups of pentaerythritol completely reacted with propargyl bromide.

Table 1. Synthesis and characterization of PE-CD and PE-CD-Br$_x$.

samples	$M_{n,\ theory}$ [a]	$M_{n,\ NMR}$ [b]	m/z [c]	$M_{n,\ SEC}$ [d]	PDI [d]
PE-CD	4931	-	4878.23	5904	1.07
PE-CD-Br$_{16}$	7315	7136	7419.03	8740	1.12
PE-CD-Br$_{48}$	12083	11306	12560.67	19320	1.15

[a]Calculated in accordance with the theory feed ratio; [b]Calculated in accordance with the ^{1}H NMR results; [c]The MALDI-TOF-MS results; [d]Molecular weights and molecular distributions (M_w/M_n, PDI) were determined by SEC using DMF as eluent relative to polystyrene standards.

Next, PE-CD was synthesized by the click reaction between PETP and an excess of CD-N$_3$. In the ^{1}H NMR spectrum of PE-CD (Fig. 2(b)), the characteristic signals for β-CD at δ=3.20-4.30, 4.40-4.90, 5.70-5.95 ppm and the proton peak of the 1, 2, 3-triazole ring at δ=7.95 ppm appeared, indicating the occurrence of the 1, 3-dipolar cycloaddition reaction. Moreover, in the FT-IR spectrum of PE-CD, the stretching vibration peak of the hydroxyl reemerged suggesting that CD terminals were bonded to the PETP-end. Meanwhile, the characteristic absorption of the azido group at 2104 cm^{-1} and those of the alkynyls at 2111 cm^{-1} disappeared, which further confirmed the complete click and removal of the unreacted CD-N$_3$. The

MALDI-TOF-MS result of PE-CD (Fig. S1 in the Supporting Information) also showed that the m/z of PE-CD + xNa^+ was 4878.23, which is quite agreement with the theory molecular weight (4931). Moreover, we also used SEC measurement to further confirm the molecular weight, although the molecular weight was somewhat larger than the actual molecular weight, but the PDI (M_w/M_n) was just 1.07. Therefore, based on above analysis PE-CD was successfully synthesized.

To graft thermoresponsive POEGMAs chains to the CD terminated PE-CD, selective esterification was first conducted on the CD moieties to introduce bromines into PE-CD. BIBB was used to react with the hydroxyl groups of β-CD. As a result, PE-CD based macroinitiators bearing several bromrines at the CD moieties were obtained. The ^{1}H NMR spectra of PE-CD-Br_x are shown in Fig. 3. Signals associated with the 2-bromoisobutyryl residue (-$C(CH_3)_2Br$) in PE-CD-Br_x were clearly discernible at δ=1.85-1.90 ppm, indicating that bromines have been successfully introduced into PE-CD. According to previous reports, due to the difference in activity among the 2, 3, 6-OHs selective modification can be fulfilled by carefully controlling the reaction conditions, normally the hydroxyls adjacent to C-2, -3 and -6 of β-CD (2, 3, 6-OH) are all able to react with BIBB during a typical esterification procedure. However, the actual conversion ratio of this reaction was not up to 100%, because bromoisobutyryl bromide is very active, and easily react with the residual H_2O in the reaction system, in order to maximum control the number of hydroxyls of CDs to react with bromoisobutyryl bromide, we first reduced the H_2O as best as we could, then added excessive amount of bromoisobutyryl bromide to PE-CD to ensure the proper ATRP macroinitiators what we wanted and designed. The best mole ratio of PE-CD to BIBB was 1:1.5x for the synthesis of PE-CD-Br_x (x≈16), 1:2.5x for the synthesis of PE-CD-Br_x (x≈48). The number average x of Br was calculated to be 15.7 and 47.5 by ^{1}H NMR based on integral ratios of resonance peaks from triazole rings at 7.95-8.0 ppm and -OCO-$C(CH_3)_2Br$ groups at 1.85-

271 1.90 ppm. The synthesis and characterization of PE-CD-Br_x are summarized in Table 1.
272 Combined the FT-IR, ^{1}H NMR, SEC, and the MALDI-TOF-MS (Fig. S2 and Fig. S3 in the
273 Supporting Information) results of PE-CD-Br_x the basic ideal ATRP macroinitiators were
274 synthesized.

275 Table 2. Synthesis and characterization of PE-CD-POEGMAs (P_1 and P_2).

samples	macroinitiator	n_{MEO2MA}:n_{OEGMA}	$M_{n,\ SEC}$ [b]	PDI [b]	LCST(^oC) [c]
P_1 [a]	PE-CD-Br_{16}	95:5	82747	1.24	41.03
P_2 [a]	PE-CD-Br_{48}	95:5	155135	1.28	43.71

276 *[a]Synthesized by the ATRP of MEO_2MA and OEGMA using PE-CD-Br_x as macroinitiators;*
277 *[b]Molecular weights and molecular distributions (M_w/M_n, PDI) were determined by SEC using*
278 *DMF as eluent relative to polystyrene standards; [c]Measured with a concentration of 1.0 mg*
279 *mL^{-1}, temperature increase at 1 ^oC min^{-1} by UV-vis spectroscopy.*

280 Using PE-CD-Br_x with 2-bromoisobutyryl active initiations as the macroinitiators, and
281 MEO_2MA and OEGMA as comonomers, star polymers, PE-CD-POEGMAs (P_1 and P_2) were
282 synthesized via ATRP, and the synthesis and characterization are summarized in Table 2. The
283 FT-IR and ^{1}H NMR spectra of PE-CD-POEGMAs are shown in Fig. 4 and Fig. 5. In the FT-
284 IR spectrum of PE-CD-POEGMAs (P_2), the stretching vibration peak of the carbonyl
285 group(C=O) increased compared with PE-CD-Br_{48}. Moreover, in the ^{1}H NMR spectrum of
286 PE-CD-POEGMAs (P_2), although the signals of 2, 3, 4, 5, 6-Hs (protons on C-2, C-3, C-4, C-
287 5 and C-6 position of β-CD) overlapped with the Hs of the methylene protons and the
288 methoxyl protons in PEG chains in the region of δ= 3.40-4.10. The characteristic signals of
289 β-CD, together with that of the 1, 2, 3-triazole ring, can also be observed at δ =4.40-4.85,
290 5.70-5.95 and 7.95, indicating that PE-CD-POEGMAs was successfully synthesized.

291 **Thermoresponsivity and morphology of PE-CD-POEGMAs**

Temperature-dependent phase transition behaviors of the PE-CD-POEGMAs aqueous solutions (1.0 mg mL^{-1}) were investigated by UV-vis spectroscopy to determine their LCSTs. PE-CD-POEGMAs were transparent with a characteristic light bluish tinge at room temperature, and upon heating gradually turned cloudy, and then the solution became white wholly but without precipitated, and the LCSTs for P_1 and P_2 were 41.03 ^oC and 43.71 ^oC, respectively. In contrast to previous reports, the difference for PE-CD-POEGMAs was that the LCSTs were higher than those linear POEGMA copolymers without CD core. This behavior might attribute to star structures and CD cores with multi-POEGMA branches affected the dehydration process of PE-CD-POEGMAs.

The potential applications of polymers in biomaterials related fields are known to be generally related to the aqueous media. Therefore, the thermoresponsivity and morphology of the synthesized PE-CD-POEGMAs in an aqueous solution were observed by DLS and TEM. The typical intensity diameter distributions of P_2 at 25 ^oC and 50 ^oC are shown in Fig. 6. At 25 ^oC, these particles with Z-average diameters of 156.8 nm with PDI=0.23 for P_2, suggested that the polymer might exist as polymeric aggregates rather than unimolecular micelles in aqueous solution, which is driven by the strong hydrophobic-hydrophilic interactions in the inner core and outer shell. While when the temperature rose above the LCST, it was found obviously that PE-CD-POEGMAs could self-assemble into more evenly nano-sized aggregates, the basically uniform aggregates formed with a Z-average diameter (DZ) of 104.3 nm with a narrow PDI of 0.072 for P_2.

To examine visually the size and morphology of PE-CD-POEGMAs, the typical TEM image of P_2 is presented in Fig. 7. Spherical micelles with a concentration of 0.2 mg mL^{-1} were found to be uniformly dispersed in the aqueous solution. These micelles, constructed from PE-CD-POEGMAs, showed light core surrounded by a black, thin corona, presenting a typical micellar characteristic, and it was apparent that the polymers appeared as uniform

particles with the diameter of 70 nm-120 nm, which was consistent with the DLS analysis. This result indicated that these micelles consist of hydrophobic PE and triazole rings as the inner core and hydrophilic POEGMA chains as the external shell. Scheme 3 summarizes the thermally-induced self-assembly behaviors for PE-CD-POEGMAs. It existed as aggregates in aqueous solutions and the thermoresponsiveness of the POEGMAs in the shell of micelles allowed a controlled phase transition into aggregates above LCST.[63-66]

Generally, polymeric micelles can be prepared by adding water to an organic solution of polymers until the required amount of water for micelle formation is obtained. However, previous reports have demonstrated that micelles can also be formed by direct dissolved amphiphilic polymers in water.[58, 59] In this work, the stable multimolecular micelles could be formed by direct dissolved PE-CD-POEGMAs into water. The self-assembly process was fast and did not require other special conditions. Therefore, this multimolecular micelle system prepared by the newly synthesized PE-CD-POEGMAs might be more fascinating. To confirm quantitatively the formation of multimolecular micelles, the CMC was estimated by fluorescence spectrophotometry using pyrene as a hydrophobic probe. The excitation spectra of pyrene in the P_2 solutions with various concentrations are shown in Fig. 8(a). The peak intensity increased and red shift was all observed with increased PE-CD-POEGMAs concentration, indicating the formation of micelles. The intensity ratio (I_{385}/I_{373}) of the pyrene excitation spectra versus the logarithm of the copolymer concentration is shown in Fig. 8(b). The CMC was obtained from the intersection of the baseline and tangent of the rapidly rising I_{385}/I_{373}, and the value was determined as 0.0043 mg mL^{-1} which further confirmed as multimolecular micelles in an aqueous solution for PE-CD-POEGMAs.

Single guest encapsulation capacities and mechanism

For PE-CD-POEGMAs, multimolecular micelles consisting of hydrophobic PE and triazole cores and hydrophilic POEGMAs shells could be easily formed in aqueous solution.

Subsequently, RB, LL, Rh and CR, common hydrophilic guest molecules were chosen for investigating the encapsulation properties of PE-CD-POEGMAs in aqueous solution. They are soluble and do fluoresce in water, and once encapsulate inside micelles, their aqueous solutions start to behave fluoresce enhancement or decrease. Except RB and CR have similar emission wavelengths, other molecules were selected because their main absorption peaks do not overlap with one another in mixed aqueous solution. Thus, their absorption intensities can be detected by fluorescence emission spectroscopy in an aqueous solution. The emission wavelengths for RB, LL, Rh and CR are 414 nm, 450 nm, 581 nm, and 417 nm, separately (Fig. S4 in the Supporting Information).

Fig. 9 represents changes of fluorescence intensities of LL and Rh depending on different concentrations of P_2, separately. The enhanced fluorescence emission intensities of LL or Rh with increase of the polymer concentration indicated that PE-CD-POEGMAs encapsulated LL or Rh in the hydrophilic shell of PE-CD-POEGMAs micelles. Similar tendency was also observed for other guest molecules (RB and CR with P_2 in Fig. S5 in the Supporting Information). All the polymeric guests (LL, RB, Rh and CR) investigated in this study were revealed a steady increase of the amount of encapsulated even at very low concentration without the presence of CMC. However, different from previous report, the above fluorescence enhancement results indicated the interactions of water soluble guests (LL, RB, Rh and CR) with the hydrophilic shell of the PE-CD-POEGMAs micelles, and also suggested that LL, RB, Rh and CR could not diffuse through the hydrophilic shell and interact with the hydrophobic micellar core. PE-CD-POEGMAs have large hydrophilic POEGMAs chains and small hydrophobic core, water soluble guest molecules were mainly encapsulated in the hydrophilic shell, which resulted in the fluorescence enhancement effect.

The encapsulation results of P_1 with LL, RB, Rh and CR are shown in Fig. S6 in the Supporting Information, It was interesting to observe that the P_1 also showed guest

encapsulation capacities, but the increases of the fluorescence intensities with increasing of the polymer concentration were obviously lower than that of P_2. While for P_2, it showed more obvious increase in the fluorescence intensity with increasing of its concentration, which indicated that P_2 can encapsulate guest molecules more efficiently. Although PE-CD-POEGMs had similar molecular structure, there were indeed existed differences for P_1 and P_2 with16 and 48 branched POEGMAs. These results indicated that the encapsulation capacities were not only dependent on the polymer concentration but also dependent on the polymer molecular structures of PE-CD-POEGMAs. [67]

Multi-guest encapsulation capacities and mechanism

Although PE-CD-POEGMAs had excellent single guest encapsulation capacities, and as the hydrophilic shell density increased the encapsulation capacities also increased. Subsequently, using the LL, RB, Rh and CR as multi-guest molecules, one-step double-guests encapsulation experiments were conducted for P_2, and the results of LL+Rh, CR+ Rh are shown in Fig. 10 and that of RB+Rh are shown in Fig. 7S in Supporting Information. The results indicated that with increased polymer concentration, the peak intensities of LL+Rh, CR+Rh, RB+Rh solutions obviously increased. Given the strong peak intensities of LL, the peak of CR or RB were wholly overlapped, therefore, only using CR+Rh+LL and CR+Rh+LL as triple-guests, the triple-guests encapsulation experiments were further conducted and the results are shown in Fig. 11. Although the peaks of CR or RB were wholly overlapped with that of LL, and the corresponding value at the top of the peaks was not observed, the peak intensities obviously increased with increased polymer concentration. This finding indicated that all guest molecules were simultaneously encapsulated into PE-CD-POEGMAs. Thus, the encapsulation property of PE-CD-POEGMAs could be applied to multi-guest molecule systems.

To further investigate the encapsulation capacity and mechanism of PE-CD-POEGMAs towards multi-guest molecules, consequently, gradual multi-guest encapsulation experiments were conducted.[58] Rh was firstly added into P_2 solution, and then LL or CR or RB was added with different amount, separately. The results of LL and CR are shown in Fig. 12 and RB is shown in Fig. 8S in Supporting Information. The results showed that the peak intensities decreased after the addition of the other guests LL, CR, RB, separately. Obviously, the encapsulation for P_2 to Rh was far to the encapsulation balance and saturation, in other words, when go on adding LL or CR or RB, P_2 would go on encapsulating the new added guest molecules. Therefore, Rh was encapsulated in the inner layer and behaved fluorescence decrease effect.

When two guest molecules were simultaneously encapsulated into the P_2 solution, then the third one was gradually added to the double guests system, and the results are shown in Fig. 13 and in Fig. 9S in Supporting Information. Taking Rh for example, when Rh+CR were simultaneously encapsulated into P_2 solution, and then LL was gradually added, the results showed that the peak intensities of Rh increased, similar result was obtained for Rh+LL with gradually added CR. While for CR+LL with gradually added Rh, the peak intensities of CR+LL behaved puzzled which was resulted from the overlapped emission wavelengths of CR and LL.

The possible explanation was that during the guest encapsulation process, both guest and host molecules would rearrange to maximize the interactions, and different guest molecules showed different synergistic encapsulation abilities based on their molecular properties.[36,68] These results further indicated that besides the molecular structures of PE-CD-POEGMAs, the synergistic encapsulation phenomenon and molecular recognition property were also the driving force. Thus, the encapsulation capacity and interaction mechanism of PE-CD-POEGMAs towards multi-guest molecules are derived from the synergistic encapsulation

phenomena of different guest molecules and the molecular recognition property of the hyperbranched structure, and the schematic representation for possible encapsulation mechanism of PE-CD-POEGMAs with single or multi-guests are shown in Scheme 3.

Conclusion

In summary, thermoresponsive amphiphilic star polymers, PE-CD-POEGMAs with PE as the central core, triazole and CD segments as the branch points, and POEGMAs as branches were synthesized by the azide-alkyne click chemistry and ATRP. The thermoresponsivity and morphology of PE-CD-POEGMAs were studied in details. The thermoresponsive PE-CD-POEGMAs showed tunable LCST behaviors in aqueous solution, and stable multimolecular micelles with the PE and triazole segments as the core and hydrophilic POEGMAs as the corona could be formed by direct dissolved PE-CD-POEGMAs into water. The encapsulation capacities of PE-CD-POEGMAs towards single and multi-guest molecules were investigated and the results indicated that water-soluble guests (RB, Rh, LL and CR) could be encapsulated by PE-CD-POEGMAs. The multi-guest encapsulation capacities of PE-CD-POEGMAs towards multi-guest molecules were derived from the molecular structure properties of PE-CD-POEGMAs and the synergistic encapsulation phenomenon of different guest molecules. As a result of their tunability of thermoresponsive behavior, easy preparation of multimolecular micelles, and potential biocompatibility they are of potential interest for applications in biomedical science.

Acknowledgements

The authors appreciate the Intergration of Industry, Education and Research of Guangdong Province project (project no. 2011A091000007), Guangdong-Hongkong Technology Cooperation Finding (project no. 2009A091300012) and National Natural Science Foundation of China (project no. 20974121). They also wish to thank professor Yu qijun

(South China University of Technology) for his support and collaboration in the test involved in this study.

REFERENCES

1 A. Hirao, R. Goseki and T. Ishizone, Macromolecules 2014, 47, 1883.

2 D. Konkolewicz, M. J. Monteiro and S. Perrier, Macromolecules 2011, 44, 7067.

3 D. Astruc, E. Boisselier and C. Ornelas, Chem. Rev. 2010, 110, 1857.

4 M. Calderon, M. A. Quadir, S. K. Sharma and R. Haag, Adv. Mater. 2010, 22, 190.

5 W. N. Xu, I. Choi, F. A. Plamper, C. V. Synatschke, A. H. E. Müller, Y. B. Melnichenko and V. V. Tsukruk, Macromolecules 2014, 47, 2112.

6 E. Zagar and M. Zigon, Prog. Polym. Sci. 2011, 36, 53.

7 H. F. Gao, Macromol. Rapid Commun. 2012, 33, 722.

8 R. Haag and F. Kratz, Angew. Chem., Int. Ed. 2006, 45, 1198.

9 L. M. Bronstein and Z. B. Shifrina, Chem. Rev. 2011, 111, 5301.

10 S. M. Grayson and J. M. J. Fréchet, Chem. Rev. 2001, 101, 3819.

11 J. H. Zhou, L. Wang, J. Z. Ma, J. J. Wang, H. J. Yu and A. G. Xiao, Eur. Polym. J. 2010, 46, 1288.

12 M. S. Rahman, M. Changez, J. W. Yoo, C. H. Lee, S. Samal and J. S. Lee, Macromolecules 2008, 41, 7029.

13 H. Mori, H. Ookuma and T. Endo, Macromolecules 2008, 41, 6925.

14 F. Liu and M. W. Urban, Prog. Polym. Sci. 2010, 35, 3.

15 C. Tsitsilianis, G. Gotzamanis and Z. Iatridi, Eur. Polym. J. 2011, 47, 497.

16 C. Weber, R. Hoogenboom and U. S. Schubert, Prog. Polym. Sci. 2012, 3, 686.

17 M. Y. Guo and M. Jiang, Soft Matter 2009, 5, 495.

18 G. S. Chen and M. Jiang, Chem. Soc. Rev. 2011, 40, 2254.

19 Y. Y. Mai and A. Eisenberg, Chem. Soc. Rev. 2012, 41, 5969.

20 M. A. Ward and T. K. Georgiou, Polymers 2011, 3, 1215.

21 B. Yu, X. S. Jiang, G. L. Yin and J. Yin, J. Polym. Sci. Part A: Polym. Chem. 2010, 48, 4252.

22 S. Yamamoto, J. Pietrasik and K. Matyjaszewski, Macromolecules 2008, 41, 7013.

23 F. Sakai, G. S. Chen and M. Jiang, Polym. Chem. 2012, 3, 954.

24 Z. S. Ge and S. Y. Liu, Macromol. Rapid Commun. 2009, 30, 1523.

25 D. Roy, J. N. Cambre and B. S. Sumerlin, Prog. Polym. Sci. 2010, 35, 278.

26 S. Han, M. Hagiwara and T. Ishizone, Macromolecules 2003, 36, 8312.

27 J. F. Lutz, O. Akdemir and H. Ann, J. Am. Chem. Soc. 2006, 128, 13046.

28 Z. X. Zhang, K. L. Liu and J. Li, Macromolecules 2011, 44, 1182.

29 B. L. Peng, N. Grishkewich, Z. L. Yao, X. Han, H. L. Liu and K. C. Tam, ACS Macro Lett. 2012, 1, 632.

30 C. R. Becer, S. Hahn, M. W. M. Fijten, H. M. L. Thijs, R. Hoogenboom and U. S. J. Schubert, J. Polym. Sci. Part A: Polym. Chem. 2008, 46, 7138.

31 O. G. Schramm, G. M. Pavlov, H. P. Erp, M. A. R. Meier, R. Hoogenboom and U. S. Schubert, Macromolecules 2009, 42, 1808.

32 E. W. Edwards, M. Chanana, D. Y. Wang and H. MÖohwald, Angew. Chem., Int. Ed. 2008, 47, 320.

33 J. F. Lutz, K. Weichenhan, O. Akdemir and A. Hoth, Macromolecules 2007, 40, 2503.

34 Y. W. Li, H. L. Guo, Y. F. Zhang, J. Zheng, J. Q. Gan, X. X. Guan and M. G. Lu, RSC Adv. 2014, 4, 17768.

35 H. Kitano, T. Hirabayashi, M. Gemmei-Ide and M. Kyogoku, Macromol. Chem. Phys. 2004, 205, 1651.

36 C. G. Mu, X. D. Fan, W. Tian, Y. Bai and X. Zhou, Polym. Chem. 2012, 3, 1137.

489 37 C. Moers, L. Nuhn, M. Wissel, R. Stangenberg, M. Mondeshki, E. B. Nicoletti, A.
490 Thomas, D. Schaeffel, K. Koynov, M. Klapper, R. Zentel and H. Frey, Macromolecules
491 2013, 46, 9544.
492 38 E. Sabadini and T. Cosgrove, Langmuir 2003, 19, 9680.
493 39 X. Y. Huan, D. L. Wang, R. J. Dong, C. L. Tu, B. S. Zhu, D. Y. Yan and X. Y. Zhu,
494 Macromolecules 2012, 45, 5941.
495 40 N. Liu, J. Vignolle, J. M. Vincent, F. Robert, Y. Landais, H. Cramail and D. Taton,
496 Macromolecules 2014, 47, 1532.
497 41 S. M. Kimani, R. L. Thompson, L. R. Hutchings, N. Clarke, S. M. Reduwan Billah, V. G.
498 Sakai and S. E. Rogers, Macromolecules 2014, 47, 2062.
499 42 X. Y. Liu, X. R. Mu, Y. Liu, H. J. Liu, Y. Chen, F. Cheng and S. C. Jiang, Langmuir 2012,
500 28, 4867.
501 43 M. Ahmed, B. F. L. Lai, J. N. Kizhakkedathu and R. Narain, Bioconjugate Chem. 2012,
502 23, 1050.
503 44 D. Steinhilber, S. Seiffert, J. A. Heyman, F. Paulus, D. A. Weitz and R. Haag,
504 Biomaterials 2011, 32, 1311.
505 45 G. B. Sun and Z. B. Guan, Macromolecules 2010, 43, 9668.
506 46 W. S. Zhuang, L. H. Liao, H. R. Chen, J. Z. Wang, Y. Pan, L. M. Zhang and D. J. Liu,
507 Macromol. Rapid Commun. 2009, 30, 920.
508 47 A. L. Sisson, D. Steinhilber, T. Rossow, P. Welker, K. Licha and R. Haag, Angew. Chem.
509 Int. Ed. 2009, 48, 7540.
510 48 T. Satoh, Soft Matter 2009, 5, 1972.
511 49 C. Ternat, G. Kreutzer, C. J. G. Plummer, T. Q. Nguyen, A. Herrmann, L. Ouali, H.
512 Sommer, W. Fieber, M. I. Velazco, H. A. Klok, J. E. Manson, Molecules, Macromol. Chem.
513 Phys. 2007, 208, 131.

514 50 G. H. Chen and Z. B. Guan, J. Am. Chem. Soc. 2004, 126, 2662.
515 51 N. Nasongkla, E. Bey, J. Ren, H. Ai, C. Khemtong, J. S. Guthi, S. Chin, A. D. Sherry, D.
516 Boothman and J. Gao, Nano Lett. 2006, 6, 2427.
517 52 H. J. Liu, Z. Shen, S. E. Stiriba, Y. Chen, W. Q. Zhang and L. H. Wei, J. Polym. Sci., Part
518 A: Polym. Chem. 2006, 44, 4165.
519 53 M. H. Stenzel, Macromol. Rapid Commun. 2009, 30, 1603.
520 54 R. Djalali, S. Y. Li and M. Schmidt, Macromolecules 2002, 35, 4282.
521 55 M. Zhang, M. Drechsler and A. H. E. Mueller, Chem. Mater. 2004, 16, 537.
522 56 K. Huang and J. Rzayev, J. Am. Chem. Soc. 2011, 133, 16726.
523 57 C. F. van Nostrum, Soft Matter 2011, 7, 3246.
524 58 W. Tian, A. L. Lv, Y. C. Xie, X. Y. Wei, B. W. Liu and X. Y. Lv, RSC Adv. 2012, 2,
525 11976.
526 59 J. Z. Du and S. P. Armes, Soft Matter 2010, 6, 4851.
527 60 F. Yao, L. Q. Xu, G. D. Fu and B. P. Lin, Macromolecules 2010, 43, 9761.
528 61 X. Wang, H. Zhang, G. Zhong and X. Wang. Polymer 2004, 45, 3637.
529 62 D. Xie, J. G. Park and J. Zhao, Dent. Mater. 2007, 23, 395.
530 63 B. W. Liu, H. Zhou, S. T. Zhou, H. J. Zhang, A. C. Feng, C. M. Jian, J. Hu, W. P. Gao and
531 J. Y. Yuan, Macromolecules 2014, 47, 2938.
532 64 Z. L. Yao and K. C. Tam, Polymer 2012, 53, 3446.
533 65 J. P. Magnusson, A. Khan, G. Pasparakis, A. O. Saeed, W. X. Wang and C. Alexander, J.
534 Am. Chem. Soc. 2008, 130, 10852.
535 66 S. T. Sun and P. Y. Wu, Macromolecules 2013, 46, 236.
536 67 H. J. Liu, Z. Shen, S. E. Stiriba, Y. Chen, W. Q. Zhang and L. H. Wei, J. Polym. Sci. Part
537 A: Polym. Chem. 2006, 44, 4165.
538 68 D. C. Wan, H. T. Pu and M. Jin, Macromolecules 2010, 43, 3809.

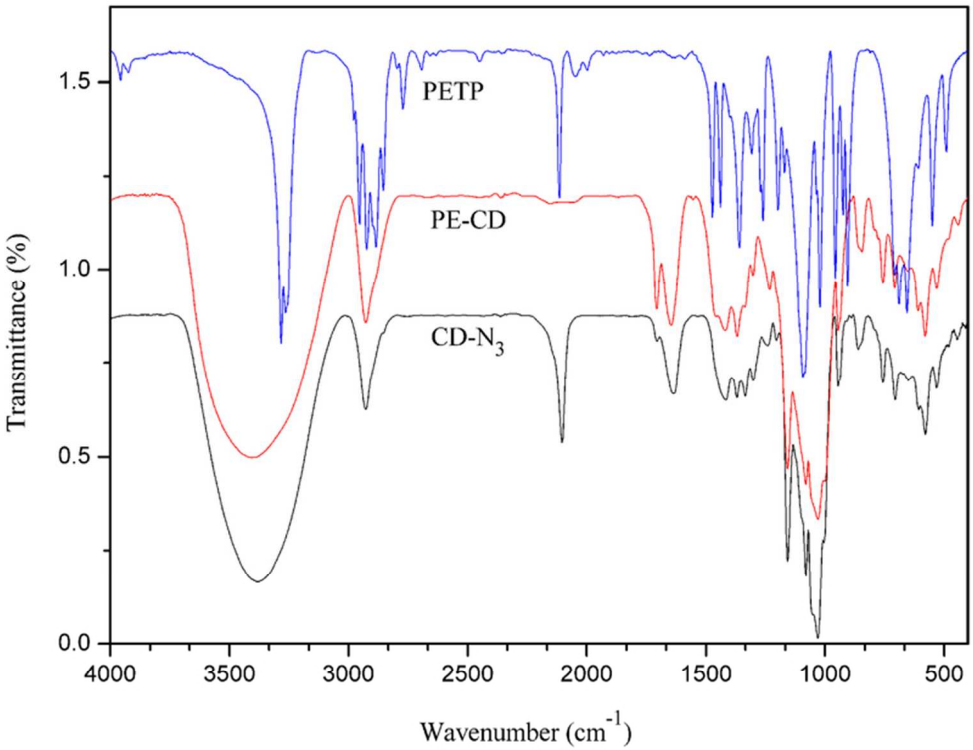

Figure 1. FT-IR spectra of CD-N3, PETP and PE-CD.
69x54mm (300 x 300 DPI)

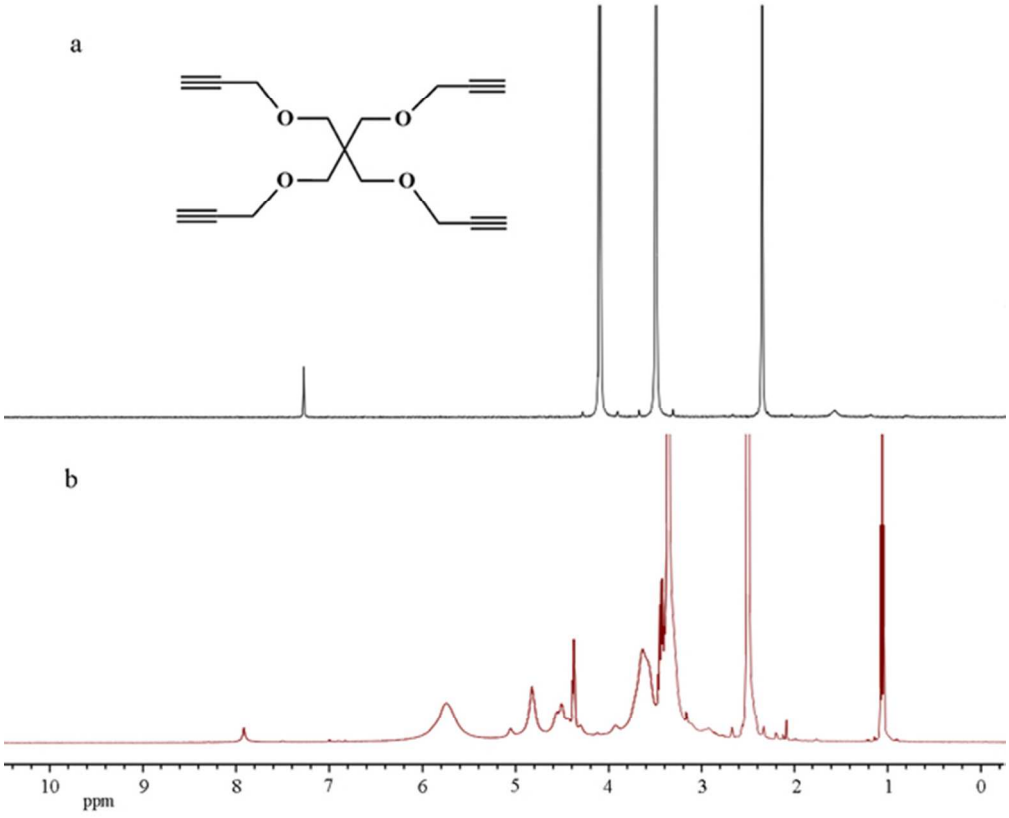

Figure 2. 1H NMR spectra of PETP (a), PE-CD (b).
55x45mm (300 x 300 DPI)

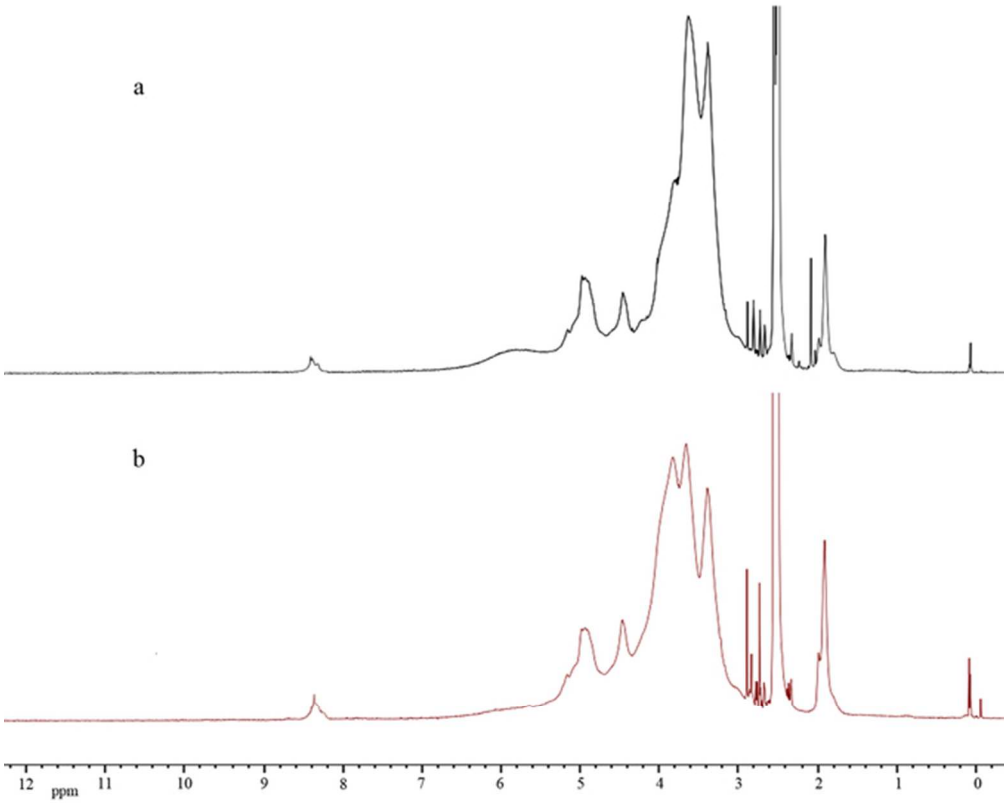

Figure 3. 1H NMR spectra of PE-CD-Br16 (a) and PE-CD-Br48 (b).
57x46mm (300 x 300 DPI)

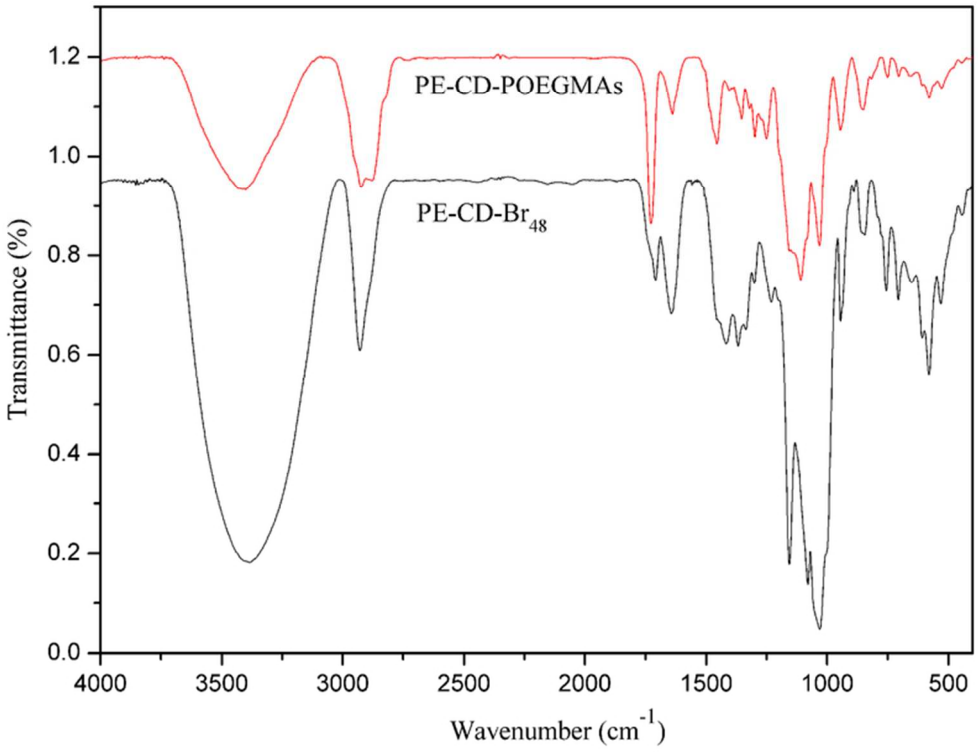

Figure 4. FT-IR spectra of PE-CD-Br48 and PE-CD-POEGMAs (P2).
68x52mm (300 x 300 DPI)

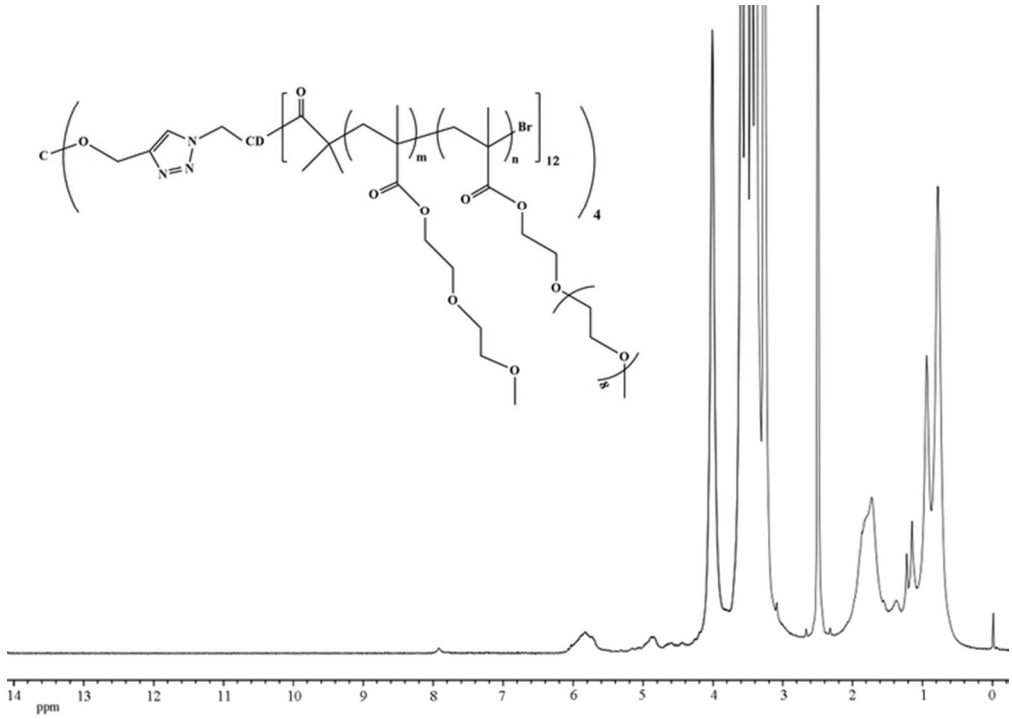

Figure 5. 1H NMR spectrum of PE-CD-POEGMAs (P2).
64x45mm (300 x 300 DPI)

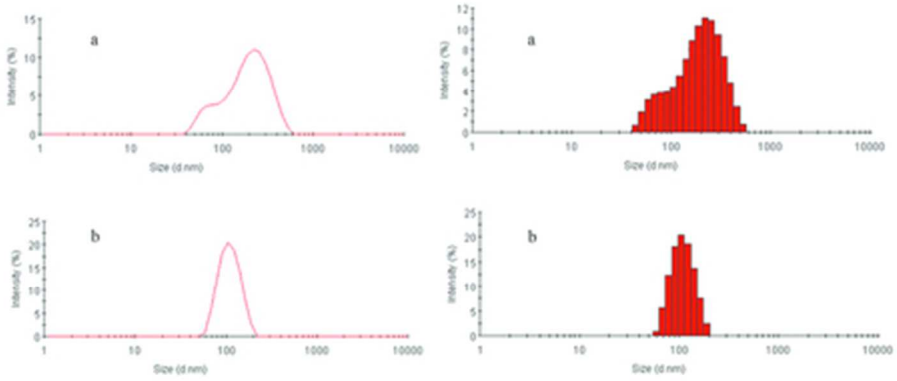

Figure 6. Size distributions of the aggregates formed by P2 in aqueous solution (0.2 mg mL-1) at 25 and 50 oC, separately.
38x16mm (300 x 300 DPI)

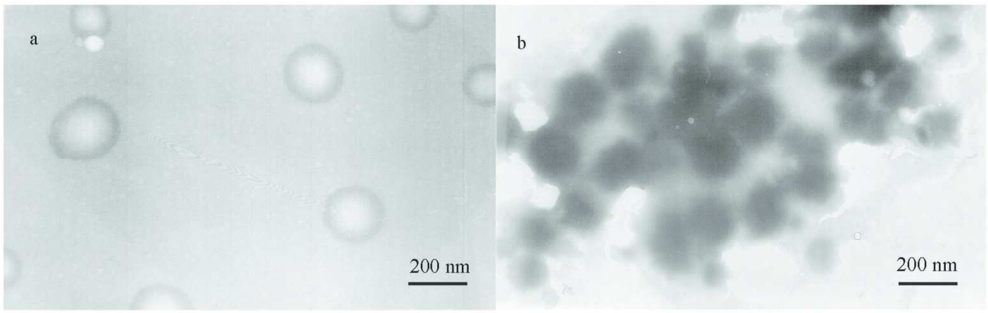

Figure 7. Typical TEM images obtained by aqueous solutions of P2 (0.2 mg mL-1) at 25 and 50 oC.
116x37mm (300 x 300 DPI)

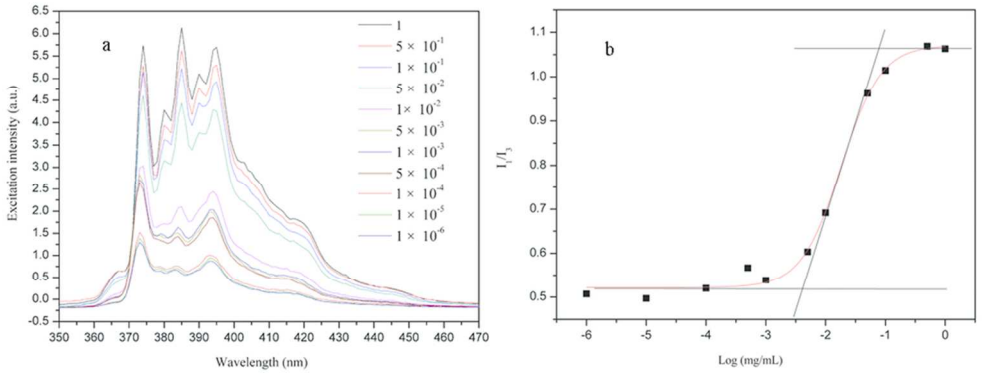

Figure 8. (a) Excitation spectra of pyrene as a function of P2 concentrations in PBS buffer (pH=7.4); (b) Plot of I385/I373 against logarithm of P2 concentration.
103x39mm (300 x 300 DPI)

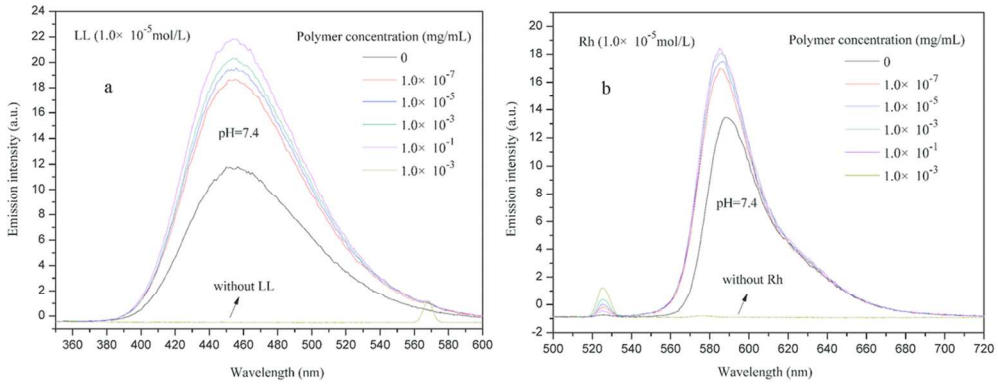

Figure 9. Fluorescence emission spectra of LL (a) and Rh (b) at pH=7.4 in the presence of different P2 concentrations.
107x42mm (300 x 300 DPI)

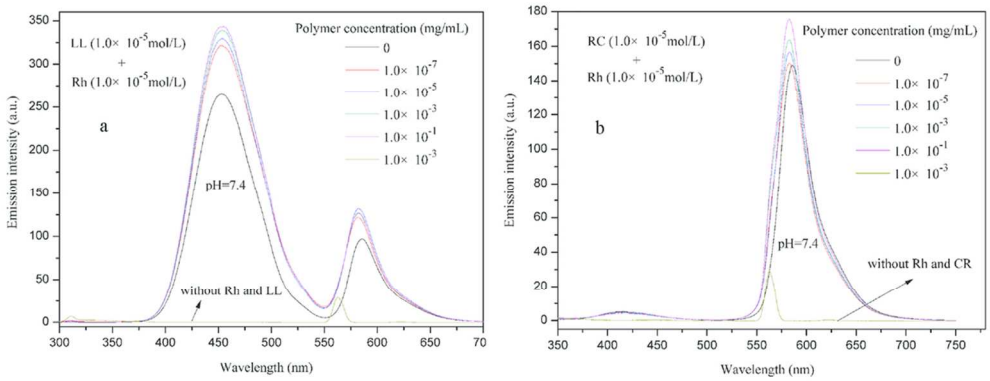

Figure 10. Fluorescence emission spectra of LL+Rh (a), and RC+Rh (b) at pH =7.4 in the presence of different P2 concentrations.
106x41mm (300 x 300 DPI)

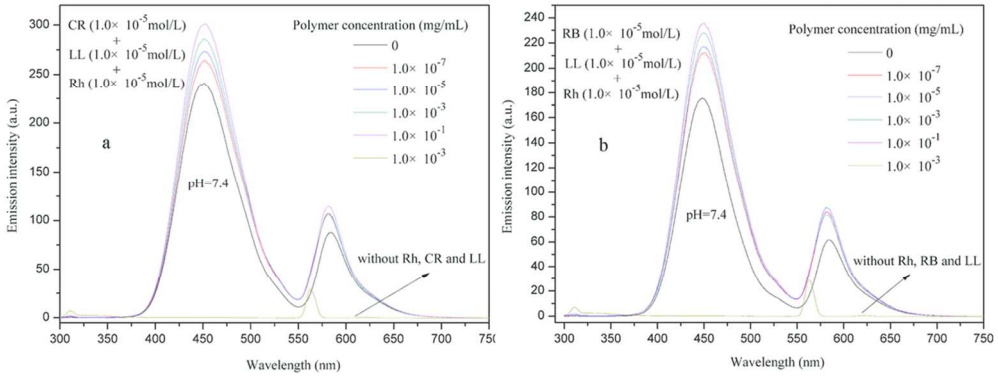

Figure 11. Fluorescence emission spectra of Rh+LL+RB (a), and RB+ LL+ Rh (b) at pH =7.4 in the presence of different P2 concentrations.
103x39mm (300 x 300 DPI)

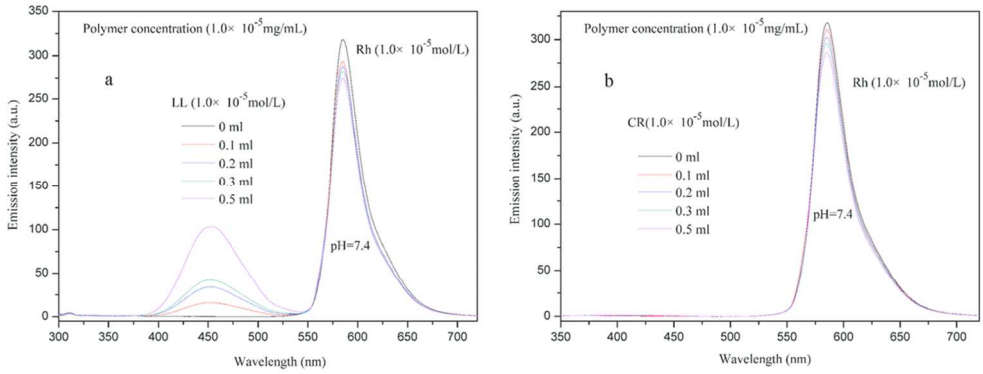

Figure 12. Fluorescence emission spectra of Rh+P2 solutions with gradual adding of LL (a) or CR (b) solutions at pH = 7.4, respectively.
101x38mm (300 x 300 DPI)

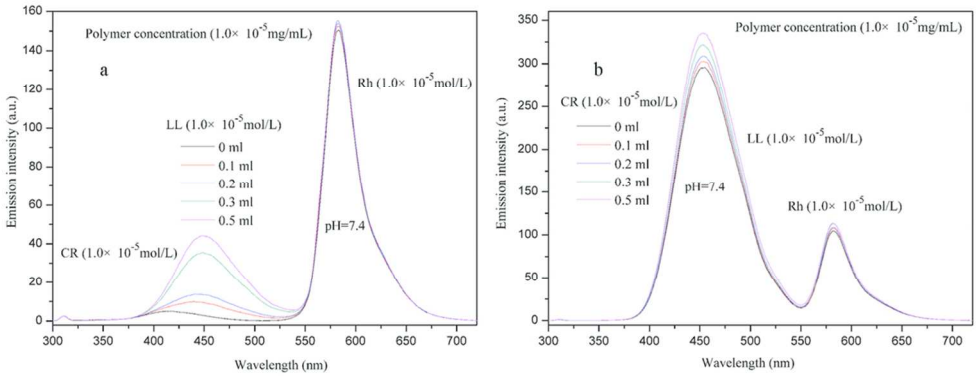

Figure 13. Fluorescence emission spectra of CR+Rh+P2 (a), LL+Rh+P2 (b) solutions with gradual adding of LL (a), CR (b) solutions at pH = 7.4, respectively.
104x40mm (300 x 300 DPI)

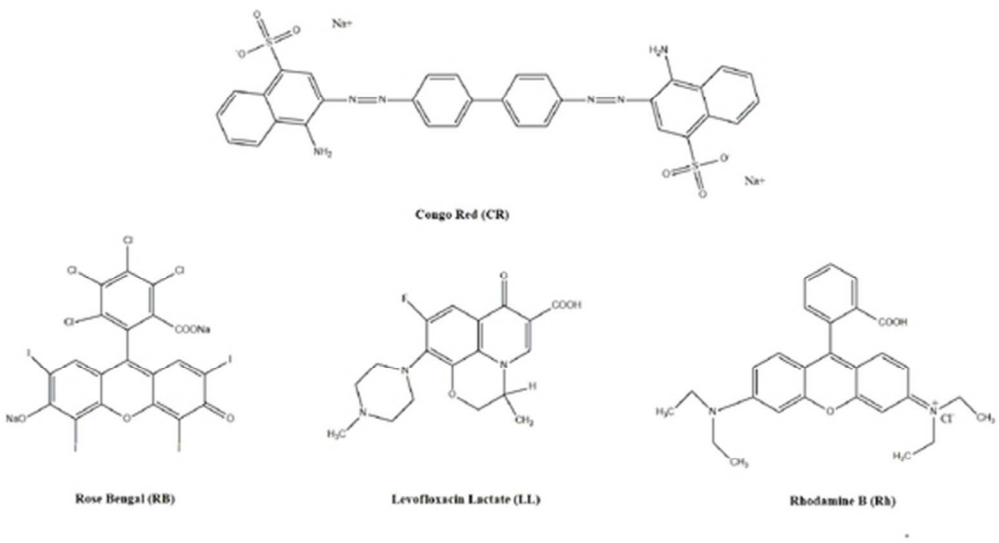

Scheme 1. The molecular structures of rose bengal (RB), levofloxacin lactate (LL), rhodamine B (Rh) and congo red (CR).
48x26mm (300 x 300 DPI)

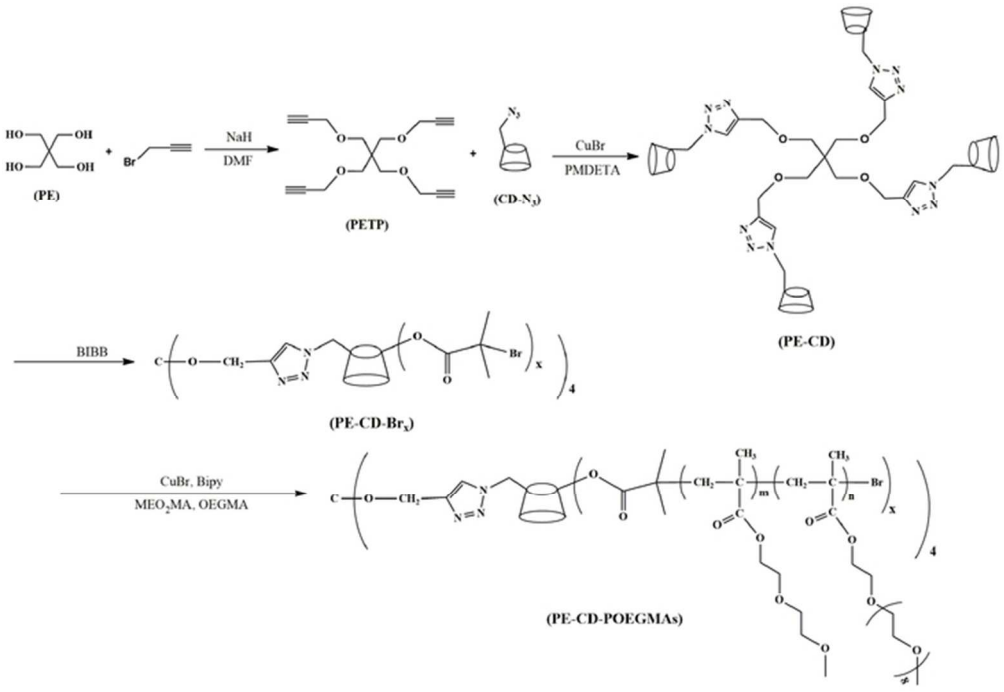

Scheme 2. The synthetic routes employed for the preparation of four arm star-shaped PE-CD-POEGMAs.
61x42mm (300 x 300 DPI)

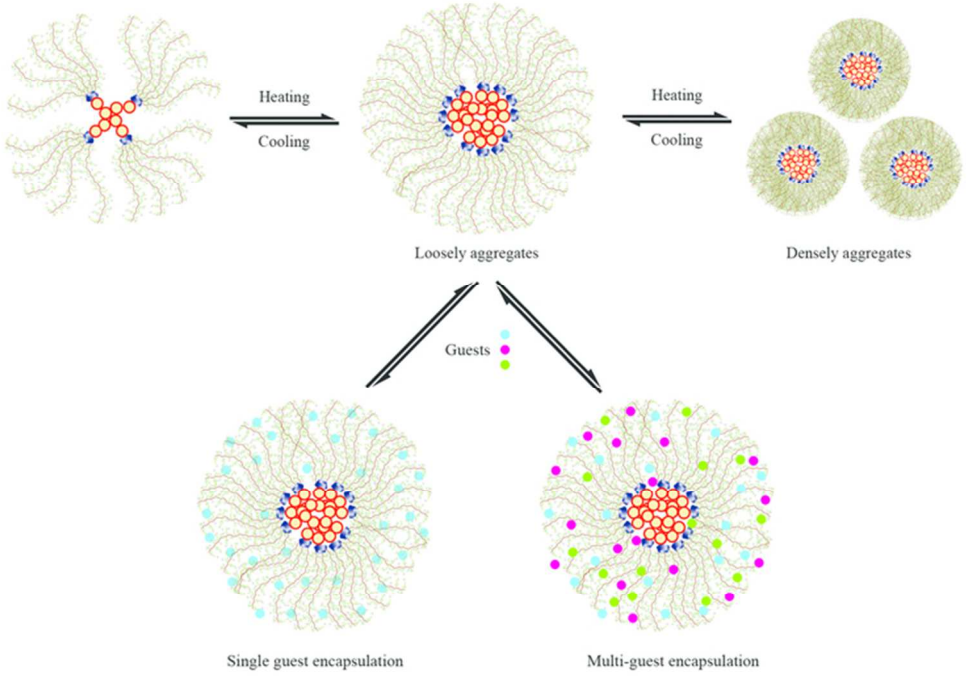

Scheme 3. Schematic illustrations of the thermally-induced self-assembly and possible encapsulation behaviors with single or multi-guests for PE-CD-POEGMAs.
64x46mm (300 x 300 DPI)